

MRS Advances © 2017 Materials Research Society. This is an Open Access article, distributed under the terms of the Creative Commons Attribution licence (<http://creativecommons.org/licenses/by/4.0/>), which permits unrestricted re-use, distribution, and reproduction in any medium, provided the original work is properly cited.

DOI: 10.1557/adv.2016.677

Creating Electrical Bistability Using Nano-bits – Application in 2-Terminal Memory Devices

Iulia Salaoru, Sattam Alotaibi, Zahra Al Halafi and Shashi Paul¹

Emerging Technologies Research Centre, De Montfort University, Hawthorn Building, The Gateway, Leicester, LE1 9BH, United Kingdom

ABSTRACT

Intensive research is currently underway to exploit the highly interesting properties of nano-bits (“nano-sized particles and molecules”) for optical, electronic and other applications. The basis of these unique properties is the small-size of these structures which result in quantum mechanical phenomena and interesting surface properties. The small molecules and/or nano-particles are selected in such a way so that it can create an internal electric in the nanocomposite. We define a nanocomposite is an admixture of small molecules and/or nano-particles and a polymer. We have demonstrated the internal electric field in our devices, made from nano-bits (nano-particles and/or molecules) and insulating materials, can contribute to the electrical bistability i.e. two conductive states.

INTRODUCTION

Memory devices play an important role in the electronics arena and inspire advances in the technologies. There has been always growing need to look for inexpensive, fast, high density and longer data retention memory devices. This work describes the use of nano-bits (nano-sized particle and small molecules) in flash-like memory devices.

Low temperature deposited materials (polymers, nano-particles small organic molecules, amorphous hydrogenated carbon (a-CH) have begun to play an important role in flexible and plastic electronics. For instance, organic materials exhibit few extraordinary properties which attract the attention of researchers and draw them a hopeful prospect for solar cells [1], thin film transistor [2], light emitting diodes [3], sensors [4] and memory devices [5-8]. We can easily demonstrate that there are a number of advantages low temperature deposited materials, for examples: materials permit to build-up devices with the high mechanical flexibility and over large areas, another one is that materials can be processable from solution form which give the opportunity to use inexpensive methods (spin coating, dip-coating, printing) at low temperature. There has been a number reports on the role of low temperature deposited materials in electronic memory devices for the last one decade [9-11]. A memory effect has been reported in a large variety of materials, including small organic molecules, nano-particles, polymers and also a variety of device and material configurations. A review article by Prime and Paul [12] discuss and differentiate among a number organic memory devices reported in the literature. Polymer memory devices (PDMs) are a class of memory devices, an admixture of polymer, nanoparticles and/or small organic molecules which exhibit two distinct electrical conductance states (low and respectively high) when the voltage is applied. These two states can be viewed as a realisation of memory devices. Polymer memory devices based on a blend of two small organic molecules (where one is an electron acceptor (A) and the second one is an electron donor (D)) and an

¹ Contact author's email: spaul@dmu.ac.uk

insulating polymer. A few research publications [13-15] have studied this type of PMDs but unfortunately, the exact working mechanism(s) is remained unclear and this leave many open questions. In 2007 [16], we had proposed a model to clarify the switching mechanism that is based on electrical dipole formation in the polymer matrix. Since then, we have applied this model to a number of different blends; by introducing deliberately electric dipoles into the system and verified if the model is still valid. Interestingly, the model does explain the observed electrical behaviour in such configuration of blends. In this work, we further investigate/scrutinised the model in-depth using optical (Fourier Transform Infra-Red spectroscopy (FTIR)) and electrical (current-voltage, retention time, capacitance-voltage testing) by deliberately creating electric dipoles in the polymer matrix using a series of electron donor (Tetrathiafulvalene (TTF), 8-hydroxyquinilone (8HQ)) and electron acceptor (tetracyanoethylene (TCNE); 7,7,8,8, tetracyanoquinodimethane (TCNQ)) small molecules, ferroelectric nano-particles (BaTiO_3) in a polymer and selenium nano-particles (Se-NPs) sandwiched between two insulating (a-C:H) layers.

These nano-bits (small molecules and ferroelectric nano-particles) are incorporated in a polymer matrix (electrically insulating) and as well as sandwiched between two insulating layers. The electrical nature of the polymer is closer to an insulating material. We also know that insulating materials do not electrically conduct and a very small amount of current (sub nA or pA) passes through them. Here is a hypothetical question- What happened, if we create an internal electrical field within the polymer matrix by some mechanism, to the current passing through the insulating layer? The magnitude of the current passing through the polymer/insulating layer can be effected by the strength and the direction of the internal applied electric field. The direction of both applied and internal electrical field will influence the magnitude of current going through the insulating layer. The “device-system” can be designed in such a way that it can result in bistability in electrical conductivity and which can then be used to realise two memory states (“0” and “1”) when a voltage is applied, thus rendering the structures suitable for data retention. These two states can be viewed as the realisation of non-volatile memory.

EXPERIMENT

Three different types of two terminal devices were fabricated using different materials to create the internal electric field; Polyvinyl acetate and BaTiO_3 blend, small organic molecules and Polyvinyl Acetate and Se-nanoparticles sandwiched between hydrogenated amorphous carbon. The following experimental sections are dedicated to each of their fabrication and testings:

(a) **BaTiO_3 + PVAc blend:** In this work, the devices were fabricated onto a glass substrate (2.25 cm^2) and on p-type silicon substrates. For Metal/Active Layer/Metal structure, firstly aluminium tracks were thermally evaporated onto a glass substrate under a vacuum pressure of about 6×10^{-6} Torr to form Al bottom contacts (2 mm wide). BaTiO_3 used in this experiment is cubic crystalline phase nanopowder, <100 nm particle size. BaTiO_3 nano-powder was annealed at 1000°C in the air for 1hour to obtain the tetragonal phase. As we know that tetragonal phase of BaTiO_3 is ferroelectric nature. Thus rendering us an internal electrical field to test our hypothesis. A polymer blend was prepared by dissolving 30mg/ml PVAc and 30 mg/ml annealed barium titanate (BaTiO_3) nanoparticles in methanol and the blend was then ultra-sonicated. Then the blend was spin-coated onto a glass substrate, which consists of Al track, at the speeds of 4000 rotations per minute (rpm). The top Al tracks were deposited on the spin-coated blend substrate as the final step in the fabrication procedure of these devices.

Metal/Insulator(blend)/Semiconductor MIS structure was formed on a p-type silicon substrate which had ohmic back contact. A blend of PVAc and BaTiO₃ nanoparticle spin-coating onto the substrate as mentioned above. Finally, Al was thermally evaporated on the top electrode. X-ray diffraction (XRD) study was conducted on both annealed and unannealed BaTiO₃ to check the phase change from cubic to tetragonal.

(b) **A blend of Small molecules and polymer:** Metal/polymer blend/metal (MPM) (Fig.-1) and Metal/insulator/blend/semiconductor (MIS) structures were fabricated and investigated. In regard to MPM structure, the polymer blend, made of polyvinyl acetate (PVAc) and two small organic molecules, was spun coated onto glass substrate marked with thin aluminium tracks, and top aluminium was evaporated onto polymer blend after the blend was dried.

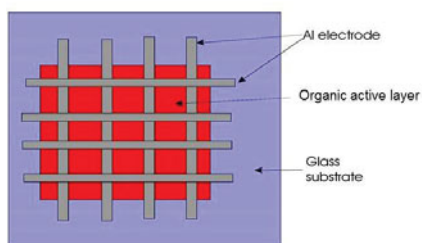


Fig-1: The cross-bar structure of Metal-Blend-Metal structure. The structure was used for testing the memory behaviour.

The MIS structures consisted of an ohmic bottom Al contact, p-type Si, a polymer blend (two small organic molecules and polystyrene (PS)), followed by polyvinyl acetate deposition and finally a top circular Al electrode.

In-depth FTIR studies were carried out to investigate charge transfer between small organic molecules. In order to carry out this study, a blend of two small organic molecules was spin-coated or drop cast directly on p-type silicon. The small organic molecules studied in this work are: 8-Hydroxyquinoline (8HQ), Tetrathiafulvalene (TTF), 7,7,8,8-Tetracyanoquinodimethane (TCNQ), Tetracyanoethylene (TCNE) and the chemical structures of them are shown in Fig.2.

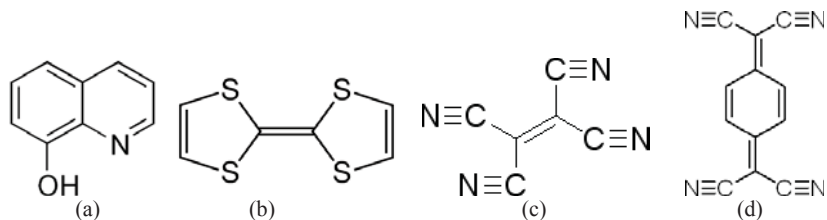


Fig-2: Chemical structures of (a) -Hydroxyquinoline (8HQ), (b)-Tetrathiafulvalene (TTF), (c)-Tetracyanoethylene (TCNE), (d)-7,7,8,8-Tetracyanoquinodimethane (TCNQ).

All small organic molecules and as well insulator polymer used in our work were purchased from Sigma Aldrich. The transmission FTIR spectra (in the spectral range 2.5-22 μm) were recorded (at room temperature) using an FTIR-8300 SHIMADZU spectrophotometer

(c) Se-Nanoparticles sandwiched between a-C:H layers: The memory device (with Se-NPs) and reference device (without Se-NPs) were fabricated by initial thermal evaporation (Edwards Auto 306 evaporator) (with base pressure 1×10^{-6} Torr vacuum, of the bottom contact electrodes (Aluminium (Al) tracks: 100 nm thick, 1 mm wide and 22 mm long) onto a flexible substrate (Lexan 8010 film is transparent polycarbonate film), then a 13.56 MHz RF PECVD was used to deposit 35nm insulating layer of the a-C:H film as blocking layer. The a-C:H film was grown at very low temperature ($\sim 40^\circ\text{C}$) using argon (Ar) and methane (CH_4) gases at a chamber pressure of 100 mTorr and radio frequency (RF) power of 100W (-80Vdc self-bias). Following this, Se-NPs were deposited at room using a vacuum evaporator. Subsequently, another dielectric film of a-C:H (8 nm thin) was deposited on top of the Se-NPs as a tunnelling layer with the same growth conditions as described for the blocking a-C:H layer. Lastly, the top Al contact electrodes were evaporated in a perpendicular direction to the bottom contacts, making out the cross-level architecture as depicted in Fig. -3

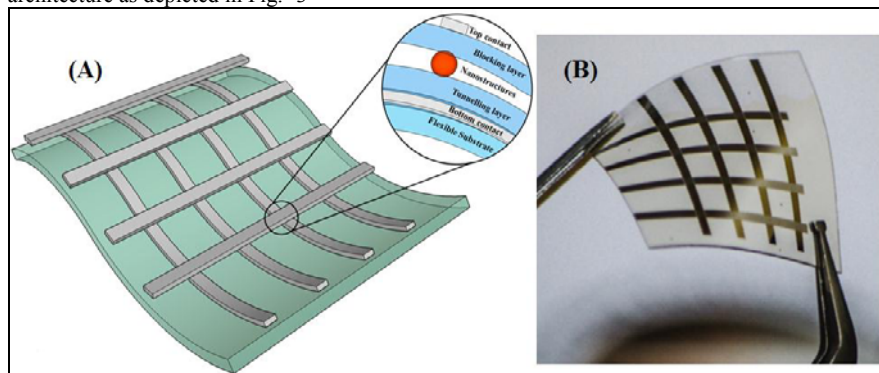


Fig.-3: (A) schematic of semi-transparent and flexible memory device and (B) photograph of fabricated semi-transparent and a flexible memory device.

Current-Voltage (I-V) and Capacitance-Voltage (C-V) measurements were conducted, for devices with and without Se-NPs devices, respectively using HP4140B pico-ammeter and an HP 4192A Impedance Analyser performed at 1 MHz frequency

RESULTS AND DISCUSSION

(a) Polymer and BaTiO_3 nano-particles blend: The annealing was carried out to change the BaTiO_3 (BTO) nanoparticles from cubic phase to tetragonal phase. The change in phase of BTO nanoparticles and the annealed sample was confirmed by XRD as shown in Fig-4.

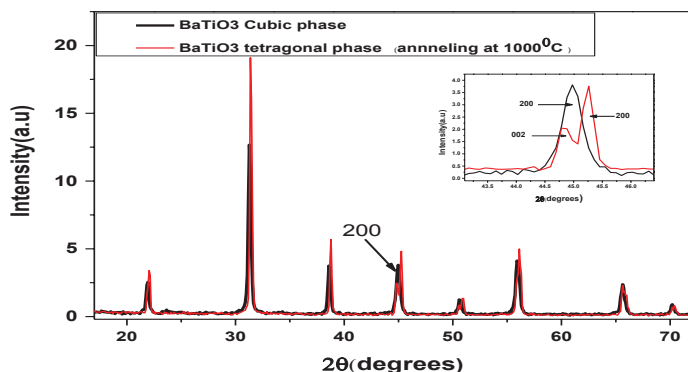


Fig-4: XRD patterns of BaTiO₃ nanoparticles as-purchased and BaTiO₃ nanoparticles annealed at 1000°C in the air. It can be observed the XRD data that the phase of nanoparticles has changed from cubic to tetragonal phase.

Polymer blend device (Al/polymer+BaTiO₃/Al) have been investigated to understand the bistability phenomenon. The structure is sandwiched between two metal conductors as is illustrated in Fig.-5 (a).

Typical $I-V$ behaviours of Al/PVAc+BaTiO₃/Al structures are shown in Fig.-5(b). In this device, $I-V$ scan exhibits large hysteresis for negative and positive applied voltages when compared with a polyvinyl acetate device. This is due to the strong internal electrical field consequence of an electric dipole associated with the tetragonal phase of BaTiO₃.

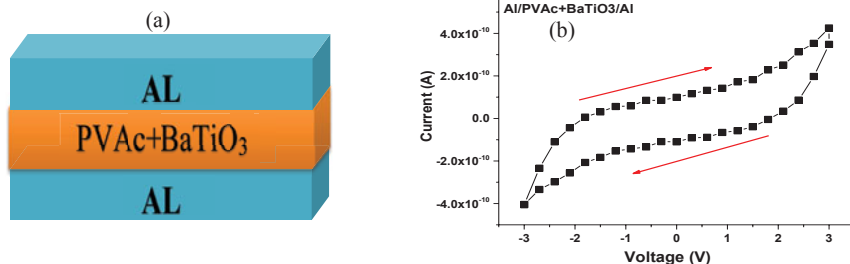


Fig.-5: (a) MIM structure. (b) Current–voltage behaviour of Al/PVAc + BTO/Al memory device.

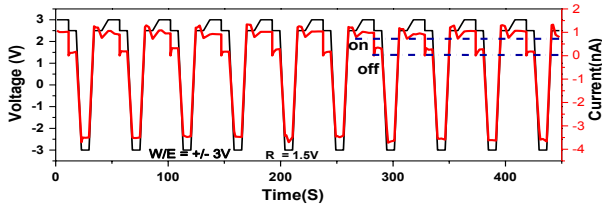


Fig-6: RWE characteristics of Al/PVAc+BaTiO₃/Al device.

The read-write-erase (RWE) cycles were carried out to investigate properties of the memory structures, with write and erase voltages of ± 3 V respectively, and a read voltage 1.5V. The RWE behaviour is shown in Fig.-6.

The device structures were further investigated by using C-V (capacitance-voltage) scans of the MIS capacitor at 1MHz frequency. The internal electric present in the memory device containing BaTiO₃ has a strong effect on the C-V hysteresis when applied voltage between -6V to +6V. MIS devices consisting of PVAc layers (not present here) demonstration a small hysteresis (0.2 V), while the MIS devices with PVAc + BTO (Fig.-7) shows a large hysteresis (3.5V), indicating that the electric dipoles (or an internal electric field present in BaTiO₃ domains) determine the bi-stable behaviour of these devices.

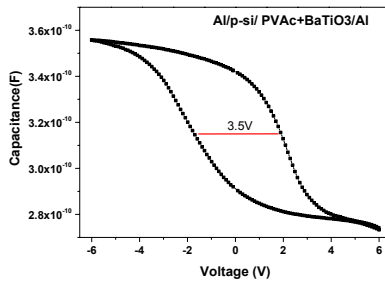


Fig.-7: C-V curves of MIS Structure (Al/p-Si/ PVAc+BaTiO₃/Al).

The capacitance-time behaviour can be used for the understanding the retention of stored information in such devices. Fig. -8 shows the bi-stable behaviour of the MIS memory test device as a function of time and the consistent difference between 0 and 1 state is around 0.62 nF for 10000 reading pulses. This argues that the device exhibited good performance.

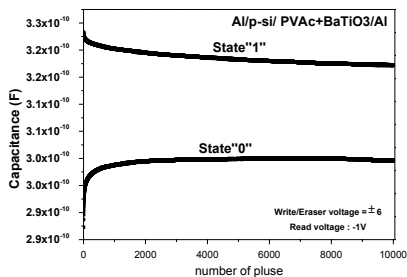


Fig-8: Typical retention time characteristics of ("0") and erased ("1") states of a memory device.

(b) **Polymer and small molecules blend:** The aim of this section of the study is to understand the working mechanism of polymer memory devices based on a blend of the polymer and two small organic molecules where one is an electron donor in the second is an electron acceptor. In our former study; we have suggested a model based on dipole formation in the polymer matrix and switching between low and conductivity state is entirely defined by the internal electric field [17-22]. Previously, we have tested our proposed model by deliberately creating electric dipoles in a polymer matrix using NaCl [18] and BaTiO₃ [19]. Although, there are a number of reports available in the literature on PMDs using donor-acceptor system, but these reports either do not explain the exact working mechanism(s) or the explanation provided fails to clarify the observed behaviour. In this work, we are investigating the properties of an admixture made up of a polymer and donor & acceptor small molecules using current-voltage, capacity-voltage and FTIR techniques. The obvious question in this study is that the results obtained from different measurement technique conclude the same phenomenon or differently.

To establish or disprove this, first of all, we investigated the infrared absorption of individual small molecules and then we investigated the IR absorption by incorporating these different donor-acceptor molecules in poly-vinyl-acetate to understand the charge transfer. In this study, a donor molecule (8HQ and TTF) and acceptor molecules (TCNE and TCNQ) were used to understanding the charge transfer using FTIR and both current-voltage and capacitance-voltages investigations were carried out to understand the observed bistability in the polymer admixtures.

The IR absorption spectra (Fig-9) of individual components of the blend (individual, small molecules) and also in the blend were recorded in the frequency range (4000-500) cm⁻¹. The formation of the charge transfer complexes is strongly sustained by monitoring the IR spectral band around 2200 cm⁻¹ which correspond to the C≡N stretching mode. In the case of pure donor molecules (8HQ and TTF) does not show any absorption around this band because these molecules do not contain C≡N triple bond. For pure electron acceptor molecules (TCNE and TCNQ) the absorption band associate with C≡N stretching occurs at 2220 cm⁻¹. The spectral band around 2200 cm⁻¹ of the charge transfer complex (blend of donor and acceptor molecules) shown a shift and as well a split of the peak (Table 1). These changes in the IR absorption spectra of a blend between small organic molecules are strongly indicating the occurrence of charge transfer between small molecules. The study of the charge transfer between various small

organic molecules have been reported other workers [23-29] and the observed results in regard to charge transfer are in line with these reports. Additionally, it is very clear from the FTIR study (Fig. -9) that the modification (splits or/and shifts) in the absorption spectra of complexes depends strongly on the types of donor-acceptor pairs.

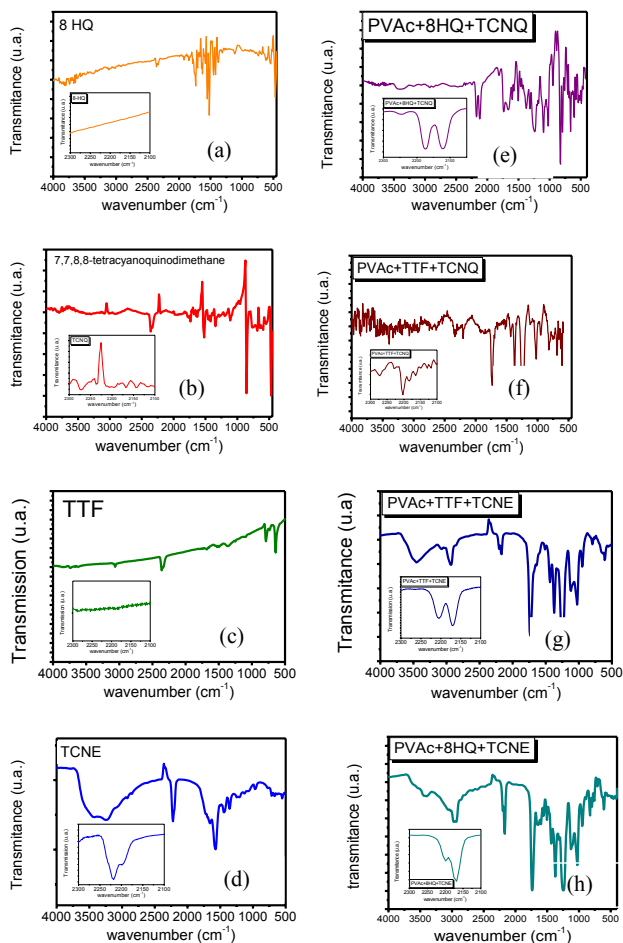


Fig.-9: IR spectra of pure components (a-d) and also donor/acceptor complexes (e-h); (a)-Hydroxyquinoline (8HQ), (b)-7,7,8,8-Tetracyanoquinodimethane (TCNQ); (c)-Tetrathiafulvalene (TTF); (d)-Tetracyanoethylene (TCNE), (e)- 8HQ-TCNQ; (f)- TTF-TCNQ; (g)- TTF-TCNE; (h)- 8HQ-TCNE.

Table 1

Charge transfer complexes	Infrared frequencies associate to 2200 cm ⁻¹ (C≡N stretching mode)	
8HQ-TCNE	2173	2196
8HQ-TCNQ	2175	2123
TTF-TCNE	2170	2203
TTF-TCNQ	2061	2200

The formation of donor-acceptor CT complexes in the polymer matrix has a great importance in understanding the function of memory devices based on them.

8HQ and TTF small organic molecules have been known as an electron donor (D) and TCNE and TCNQ as an electron acceptor (A) [23,24]. When an electron donor and electron acceptor molecules are embedded in the polymer matrix the charge carriers (electrons) go from donor molecules (results in D⁺) into the electron acceptor molecules (results in A⁻) and polymer matrix help to retain the charge in it. In this way, one can create electric dipoles in the polymer matrix and the dipole formation leads to an internal electric field. The fundamental principle of non-volatile memory devices is based on the existence of two conductivity states (low and high) respectively, and switching between them at certain applied voltage (write and erase voltage respectively). Correlate with this principle, our devices will be in the low conductivity state when the direction of the internal electric field is opposite to the external electric field and will be in the high conductivity state when both externally applied electrical field and internal electric field (due to the dipole formation in the polymer matrix) will be in the same direction. Previously, we have proposed the model based on electrical dipole formation [21,22].

Memory behaviour of four different types (different donor-acceptor complexes) was investigated by recording current-voltage characteristics, as shown in Fig.-10.

Fig.-10 shows the hysteresis in the I-V behaviour of different combinations of donor-acceptor pairs in PVAc. The sample without small molecules Al/PVAc/Al (not shown here) illustrate a small hysteresis as compared to the devices fabricated from a blend of two small molecules. The device starts in the high conductivity state and after that at certain voltage – write voltage will be switched in the low conductive state where it will remain before to apply the erase voltage. Write and erase voltage were then selected to prevent any physical damage of the samples during the testing (generally, lower than the breakdown voltage). The read voltage was selected to be the point where the maximum difference in the hysteresis.

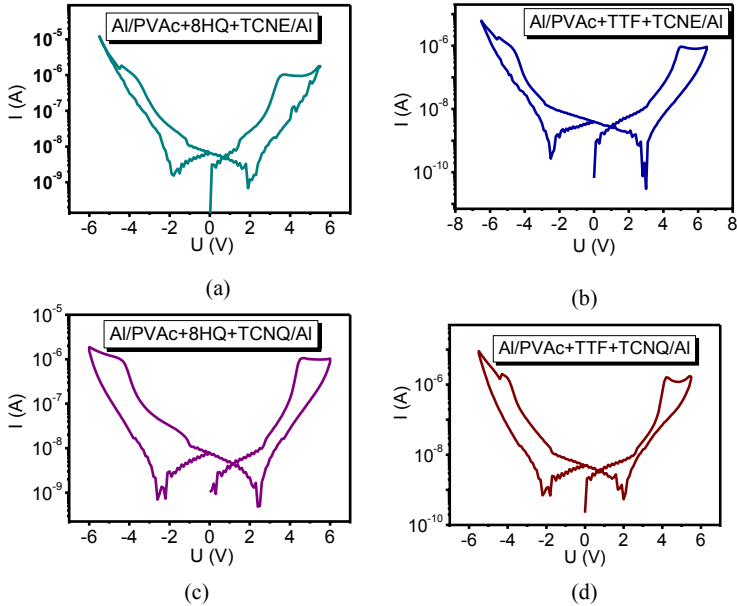


Fig.-10: Current-voltage characteristics of (a) Al/PVAc+8HQ+TCNE/Al; (b) Al/PVAc+TTF+TCNE/Al; (c) Al/PVAc+8HQ+TCNQ/Al; (d) Al/PVAc+TTF+TCNQ/Al;

The values of write/erase, reading voltage and of current in the high and low conductivity states are shown in Table 2.

Table 2

Charge –transfer complex	Write/erase voltage (V)	Read voltage (V)	Current in the high state (A)	Current in the low state (A)
8HQ-TCNE	(5.5/-5.5)	4	$1.3 \cdot 10^{-6}$	$3.3 \cdot 10^{-7}$
8HQ-TCNQ	(6/-6)	5	$1.0 \cdot 10^{-6}$	$1.2 \cdot 10^{-7}$
TTF-TCNE	6.5/-6.5	5.5	$1.7 \cdot 10^{-6}$	$4.0 \cdot 10^{-7}$
TTF-TCNQ	5.5/-5.5	5	$1.2 \cdot 10^{-6}$	$3.1 \cdot 10^{-7}$

Table-2 shows an order magnitude difference of the current values in the high and low conductivity states.

The stability is an important issue in PDMs performance. In this regard, we have investigated the effect of continuous read pulses on the high and low states for a period of over 4 hours. It is clear from Fig.-11 that the devices exhibiting distinguishable conductivity states over 4h and after that of continuous operation there was a decline in both ON and OFF state after some time, more accentuate especially of the high state.

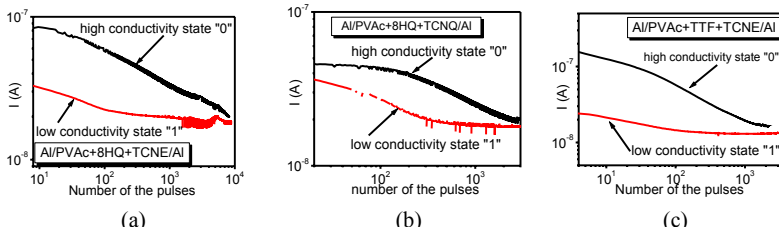


Fig-11: Retention time of (a) Al/PVAc+8HQ+TCNE/Al; (b) Al/PVAc+8HQ+TCNQ/Al; (c) Al/PVAc+TTF+TCNE/Al nano-composite blends.

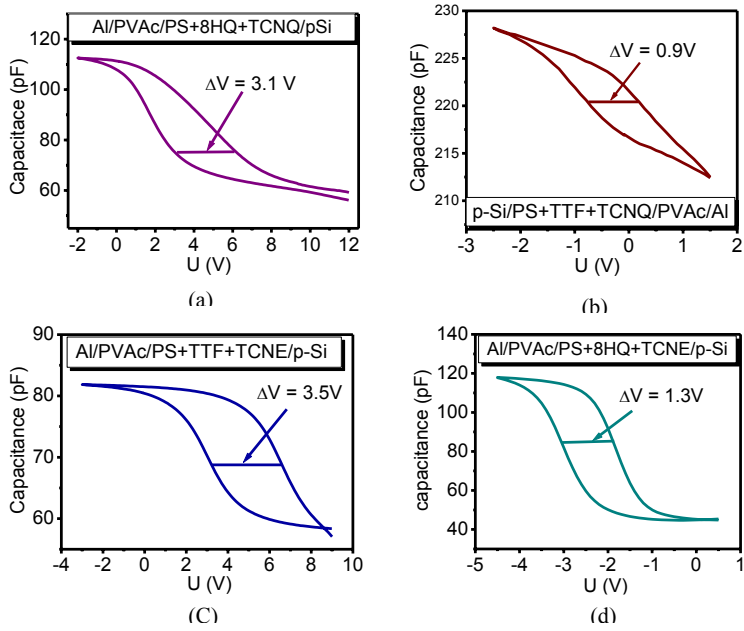


Fig-12: Capacitance-voltage characteristics of (a) Al/PVAc/PS+8HQ+TCNQ/p-Si; (b) Al/PVAc/PS+TTF+TCNQ/p-Si; (c) Al/PVAc/PS+TTF+TCNE/p-Si; (d) Al/PVAc/PS+8HQ+TCNE/p-Si;

In order to confirm that small organic molecules play a vital role in the switching mechanism in our devices the capacitance-voltage (C-V) measurements were carried out.

The C-V curve for the pristine sample (without small molecules) and also for all organic molecule pairs (donor-acceptor) embedded in the polymer matrix shows accumulation-depletion-inversion regions which are typical for MIS structures. The C-V behaviour for the samples based on an admixture of two small organic molecules (one is an electron donor and the second is an electron acceptor) in the polymer matrix reveal a large hysteresis are presented in Fig.-12. For pristine Al/PVAc/PS/Si (p-type) sample (is not shown here) the capacitance-voltage characteristics show a flat hysteresis (0.2V) All these results suggested that the dipole is created in the polymer matrix and that bistability of the devices are completely determined by internal electric field.

It is evident that all MIS device investigated have shown a very clear hysteresis loop and that the magnitude of threshold voltage depends upon the nature of electron acceptor and donor selected to form the CT pairs and also on the concentration and the ratio of them in the blend.

(c) Se-Nanoparticles sandwiched between a:C:H layers: I-V measurements were carried out on a reference device (without Se-Nps) and a memory device(with Se-NPs), to investigate the charge storage in Se-NPs. The voltage was swept from -5V to +5V on Se-NPs memory and reference device as shown in Fig.-13, the arrows refer to the direction of the sweep. The structure of memory device is Al/a-C:H/SeNs / a-C:H /Al, where Se-NPs can be deposited by a simple, low cost vacuum thermal evaporation process without the need for further optimisation at room temperature on flexible substrates. The structure of reference device is Al/a-C:H / a-C:H /Al. However, the device containing SeNPs shows a large hysteresis that is 2.5 times larger than the hysteresis showed by the reference device. Moreover, the measured current difference between the low and high conduction state at +0.5V is around 750pA, as depicted in curve (2) of Fig.-13. Whereas a relatively small difference in measured current is observed for the reference device as shown in the loop (1) of Fig.-13. This is attributed to the ability of Se-NPs to serve as a storage medium; this is confirmed by measuring hysteresis in an I-V curve that reflects in the electrical behaviour of the charges stored in Se-NPs.

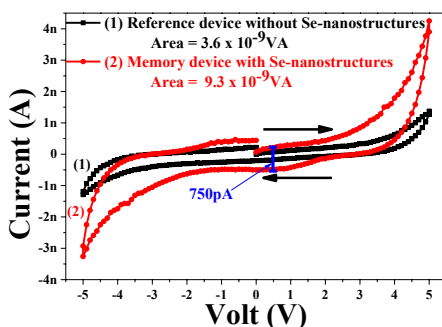


Fig.-13: I-V characteristics of devices without (loop (1)) and with (loop (2)) Se-NPs on Flexible substrates.

In order to confirm tunnelling of charges (electrons) in SeNs at applied a high voltage, several sweep voltages are applied (± 1 , ± 2 , ± 3 , ± 4 and $\pm 5V$) on memory devices containing Se-NPs [30]. These I-V measurements show symmetrical characteristics for each sweep process, as shown in Fig.-14. The fact that the area of hysteresis increases when the I-V sweep is changed, is due to enhanced tunnelling that provides more charges to store in Se-NPs. On the basis of this observation, we believe that there are more charges injected possible due to tunneling mechanism when applied voltage is increased. Hence, the enclosed area can be used as a vital parameter which refers to the amount of stored charge [31-32]. Fig.-14 suggests a consistent dependence of increased area with respect to the sweep voltage. Further investigation is currently underway, in our lab, to rule out any other charge storage mechanism.

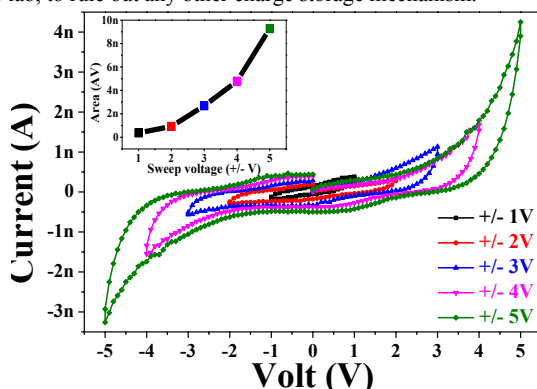


Fig.-14: I-V characteristics of the memory device at different sweep voltages. The inset shows the change in the area surrounded by the hysteresis Vs scan voltage maximum value when the voltage range is varied. The trend in the graph also suggests the charge storage in Se-NPs is a non-linear function of the maximum value of the scan voltage.

CONCLUSIONS

We have clearly proven that by fabricating three different types two terminal devices, we can produce an internal electrical field. The internal electric field is the sole contributor to the electrical bistability in such devices. If the internal electrical field can be maintained, by designing the proper material system, we will able to improve the retention time.

ACKNOWLEDGEMENT

The authors (IS and SP) would like to thank EPSRC (Grant #EP/E047785/1) for supporting this work.

Contributions:

IS conducted the experiment and analysis related to small molecules & polymer blend and drafted the section related to it. ZH conducted the experiment and drafted the section related to BaTiO₃ and Polymer blend. SA conducted the experiment and drafted the section related Se nano-particles section. IS and SP contributed in re-writing the manuscript. The testing of charge

transfer between donor and acceptor molecules, by FTIR, was IS' idea. The idea of the creation of an internal electric field and use it for memory devices was conceived by SP.

References:

- [1] S. Subianto, N.Dutta, M.Andersson, N.R.Choudhury, Adv. Colloid. and Interface Science 235 (2016) 56. [2] J.Soeda, T.Okamoto, C.Mitsui, J.Takeya, Organic Electronics: physics, materials, applications 39 (2016) 127.
- [3] D.Riedel, T.Wehlus, T.C.G. Reusch, J.Brabec Organic electronics 32 (2016) 27
- [4] P.J.Jeon, K.Lee, E. Young Park, S. Im, H.Bae, Organic electronics, 32 (2016) 208.
- [5] K.Ran, B.Rosner, B.Butz, R.H.Fink, E.Spiecker, Nanotechnology 27 (42) (2016) 425703
- [6] T.Leydecker, M.Herder, E.Pavlica, G.Bratina, S.Hecht, E.Orgiu, P.Samori, Nature Nanotech., 11(9) (2016) 769
- [7] Y.Liu, F.Li, Z.Chen, T.Guo, C.Wu, T.W.Kim, Vacuum 130 (2016) 109. T.Wei, G.Chen,
- [8] H-Y Tsao, Y-W Wang, Z-K Gao, Thin solid Films 612 (2016) 61
- [9] M-G. Kim, M.G.Kanatzidis, A.Facchetti, T.J.Marks, Nat. Materials, 10 (2011) 382
- [10] K.Zhang, L.Hao, M.Du, J.Mi, J.N.Wang, J-P. Meng, Renewable and sustainable energy 67 (2017) 1282.
- [11] J.Socratous, K.K.Banger, Y.Sadhanata, A.D.Brown, A.Sepe, U.Steiner, H.Sirringhaus, Adv.Funct.Mater., 25 (2015) 1873.
- [12] D.Prime, S.Paul, Phil.Trans.R.Soc.A, 367(1905) (2009) 4141.
- [13] C.W.Chu, J.Ouyang, J.H.Tseng, Y.Yang, Adv.Mater. 17 (2005) 1440.
- [14] J.R.Koo, S.W.Pyo, J.H.Kim, S.Y.Jung, S.S.Yoon, T.W.Kim, Y.H.Choi, Y.K.Kim, Synth.Metals, 156, (2006), 298,
- [15] Y.Ma, X.Cao, G.Li, Y.Wen, Y.Yang, J.Wang, S.Du, L.Yang, H.Gao, Y.Song, Adv.Funct.Mater., 20, (2010), 803
- [16] S Paul, IEEE Transactions on Nanotechnology 6 (2007) 191.
- [17] I.Salaoru, S.Paul, Journal Optoelectronics and Advanced Materials 10(12) (2008) 3461.
- [18] I.Salaoru, S.Paul, Advances in Science and Technology 54 (2008) 486.
- [19] I.Salaoru, S.Paul, Phil.Trans.R.Soc.A, 367(1905) (2009) 4227.
- [20] I.Salaoru, S.Paul, Mater. Res. Soc. Symp. Proc., 1114-G12-09 (2009).
- [21] I.Salaoru, S.Paul, Mater. Res. Soc. Symp. Proc., 1250-G07-11 (2010).
- [22] I.Salaoru, S.Paul, Thin Solid Films, 519 (2010) 559
- [23] D.A.Clemente, A.Marzotto, J.Mater.Chem. 6(6) (1996) 941.
- [24] M.Meneghetti, C.Pecille, J.Chem.Phys. 105(2) (1996) 397.
- [25] M.Meneghetti, C.Pecile, Synthetic Metals 86 (1997) 2037.
- [26] D.A.Clemente, C.Pecile, Molecular Crystals and Liquid Crystals, 121(1-4) (1985) 397.
- [27] M.R.Bryce, Advanced Materials 11(1) (1999) 11.
- [28] M.R.Bryce, W.Devonport, L.M.Goldenberg, C.Wang, Chem. Commun. 945 (1998)
- [29] J.S.Miller, Angew.Chem.Int.Ed. 45 (2006) 2508.
- [30] S. Alotaibi, N. Gabrielyan and S. Paul Advances in Science and Technology, vol. 95, pp. 100-106, 2014.
- [31] E. H. Nicollian, J. R. Brews and E. H. Nicollian, *MOS (Metal Oxide Semiconductor) Physics and Technology*. Wiley New York et al., 1982.
- [32] K. Saranti, S. Alotaibi and S. Paul, Sci. Rep., vol. 6, pp. 27506, Jun 9, 2016.